



# Sediment dynamics shape macrofauna mobility traits and abundance on tidal flats

Zhengquan Zhou <sup>1,2,3\*</sup> Tim J. Grandjean,<sup>1,2</sup> Jaco de Smit,<sup>4</sup> Jim van Belzen,<sup>1,5</sup> Gregory S. Fivash <sup>1,6</sup>  
Brenda Walles,<sup>4</sup> Olivier Beauchard,<sup>1</sup> Jeroen van Dalen,<sup>1</sup> Daniel B. Blok,<sup>1</sup> Lennart van IJzerloo,<sup>1,2</sup>  
Tom Ysebaert,<sup>1,5</sup> Tjeerd J. Bouma<sup>1,2,4</sup>

<sup>1</sup>Department of Estuarine and Delta Systems, NIOZ Royal Netherlands Institute for Sea Research, Yerseke, The Netherlands

<sup>2</sup>Department of Physical Geography, Faculty of Geosciences, Utrecht University, Utrecht, The Netherlands

<sup>3</sup>The Swire Institute of Marine Science and Area of Ecology and Biodiversity, School of Biological Sciences, The University of Hong Kong, Hong Kong SAR, China

<sup>4</sup>Building with Nature Research Group, HZ University of Applied Sciences, Middelburg, The Netherlands

<sup>5</sup>Wageningen Marine Research, Wageningen University and Research, Yerseke, The Netherlands

<sup>6</sup>Ecosphere Research Group, Department of Biology, University of Antwerp, Antwerp, Belgium

## Abstract

Tidal flats are valuable ecosystems that depend on complex biogeomorphic processes between organisms and sediment transport. Climate change has led to a rise in extreme weather events, such as storms. This, in turn, has increased sediment dynamics and created risks for the benthic communities inhabiting tidal flats. However, replicating sediment disturbances caused by extreme weather is difficult. To overcome this, we used the plow rake to enhance the natural tidal currents and wave conditions to simulate intensified sediment dynamics. The raking disturbance was repeated on two intertidal zones with different inundation frequencies and wind fetch levels to simulate the increasing frequency of storm impact on sediments due to climate change. We compared the measurements of sediment dynamics and macrofauna between plots that were raked and the control plots that were only influenced by natural hydrodynamics. Results showed that tidal flat sediments experienced erosion by 10–20 mm after six times biweekly raking treatments, depending on the site-specific hydrodynamic conditions. Sediment dynamics served as a helpful tool for monitoring the species distribution regarding mobility traits: the high dynamic exposed sites were inhabited by mobile species, while the low dynamic sheltered sites were characterized by less-mobile species. Moreover, the raking treatment decreased the abundance of species with immobile traits, yet the species composition did not experience significant change. Overall, the present findings indicate that tidal flats with low sediment dynamics and immobile macrofauna are at higher risk of declining abundance under intensified sediment disturbances than areas with high sediment dynamics and mobile macrofauna.

Benthic organisms play important roles in intertidal ecosystems, contributing significantly to the depositional environment through various physical and chemical pathways (Meysman et al. 2006; Murray et al. 2002). The physical stabilization of

intertidal deposits is predominantly attributed to the presence of microphytobenthos that release biofilms, as well as the activities of organisms that construct epibenthic structures such as tubes or reefs (Borsje et al. 2014; Walles et al. 2015). These biofilms

\*Correspondence: [zhengquan.zhou@nioz.nl](mailto:zhengquan.zhou@nioz.nl)

Additional Supporting Information may be found in the online version of this article.

This is an open access article under the terms of the [Creative Commons Attribution-NonCommercial](https://creativecommons.org/licenses/by-nc/4.0/) License, which permits use, distribution and reproduction in any medium, provided the original work is properly cited and is not used for commercial purposes.

**Author Contribution Statement:** ZZ: Conceptualization; Investigation; Methodology; Data curation; Formal analysis; Visualization;

Writing – original draft preparation; Writing – review and editing. TJG: Conceptualization; Methodology; Data curation; Formal analysis; Visualization; Writing – review and editing. JdS: Conceptualization; Investigation; Methodology; Data curation; Formal analysis; Writing – review and editing. JvB: Conceptualization; Visualization. GSF: Data curation; Formal analysis; Writing – review and editing. BW: Conceptualization; Investigation; Methodology; Writing – review and editing. OB: Data curation; Formal analysis; Writing – review and editing. JvD: Investigation; Methodology. DBB: Investigation; Methodology. Lvl: Investigation; Methodology. TY: Conceptualization; Investigation; Methodology. TJB: Conceptualization; Methodology; Visualization; Supervision; Project administration; Funding acquisition; Writing – review and editing.

and structures play important roles in safeguarding the sediment against the erosive impact of the hydrodynamics (Wright and Jones 2006; Le Hir et al. 2007). Conversely, sediment destabilization is often a result of *bioturbation*, a process in which the behavioral traits of benthic organisms actively lead to sediment transport (Meysman et al. 2006; Kristensen et al. 2012).

The biological traits of benthic macrofauna are significantly influenced by abiotic factors (van der Wal et al. 2017), and changes in the trait composition are frequently utilized to assess how the macrobenthic community reacts to environmental pressures, including both natural and anthropogenic processes (Bremner et al. 2006; van der Linden et al. 2012). Biological traits enable species to adapt and reproduce in specific conditions, thereby defining their niche breadth: the spectrum of environmental conditions and resources that a species can tolerate and utilize (McLachlan and Defeo 2018a). For instance, in the context of tidal flat macrofauna, traits related to mobility, feeding strategies, and reproduction can significantly affect a species' ability to withstand varying environmental gradients, such as exposure to wave action and sediment characteristics (McLachlan and Defeo 2018b). The World Register of Marine Species (WoRMS) has become an invaluable resource in this context, standardizing marine species traits and providing a comprehensive database for marine ecology studies (WoRMS Editorial Board 2024). The WoRMS traits and modalities categorize different aspects of the physiology, life styles, and behaviors of various species, which aids in comparisons across different taxa.

Mobility traits, such as burrowing ability, play a crucial role in enabling species to avoid predation and adapt to sediment movement (Romano et al. 2011; MacDonald et al. 2014). However, species' abilities often involve trade-offs; specialization in one trait may compromise the performance in another (Shoval et al. 2012; Garland 2014). For instance, a species with high mobility might be more vulnerable to predation or less adept at exploiting localized resources (Gu et al. 2006). The complex interaction between mobility traits and environmental dynamics, particularly sediment movement, greatly affects the overall fitness and distribution of macrofauna in their habitats (Thrush et al. 1996; Soissons et al. 2019).

Unvegetated tidal flats, which serve as habitats for benthic organisms, are dynamic ecosystems that experience various environmental pressures and biogeomorphic feedback influenced by hydrodynamic forces (van de Koppel et al. 2001; Fagherazzi et al. 2013). Despite their ecological significance, tidal flats have declined in total area globally by 16% between 1984 and 2016, primarily attributed to the combined impacts of climate change and human activities (Murray et al., 2002). Consequently, these crucial ecosystems are becoming increasingly vulnerable to the impacts of extreme storm events (FitzGerald et al. 2008; Cazenave and Cozannet 2014; Hinkel et al. 2014). Storms have the potential to significantly amplify tidal amplitudes and increase current speeds, resulting in substantial sediment erosion and

resuspension events (Janssen et al. 2019; Zhu et al. 2020; de Vet et al. 2020). These events intensify the sediment dynamics within intertidal flats and impose severe and irreversible consequences on the benthic organisms that rely on these habitats (Naeem et al. 1994; Shi et al. 2021).

Several studies indicate that enhanced sediment dynamics caused by storms decrease the overall population of benthic macrofauna (Bouma et al. 2001; Shi et al. 2021). According to Shi et al. (2021), the occurrence of a typhoon over 1400 km away could cause sediment erosion of up to 10 cm and lead to a decline of nearly 50% in both the abundance and the biomass of clams inhabiting the tidal flats. Bouma et al. (2001) also demonstrated that sediment dynamics can significantly impact the passive resuspension of early recruits, and the existence of low-dynamic zones is crucial for the establishment of bivalve populations during their initial recruitment stage. In this study, we focus on the daily sediment dynamics of tidal flats, that is, the temporary changes in the surface elevation caused by the interaction between tidal patterns and other factors, such as wind and wave action, that disrupt the dynamic equilibrium (Hu et al. 2017; Grandjean et al. 2023).

Although it is known that increased sediment dynamics, either from normal conditions or storms, can negatively affect benthic organisms, there is still uncertainty about how daily sediment dynamics can shape the biological traits and community structures of benthic macrofauna. The relationship between sediment dynamics and the biological traits of macrofauna is crucial for enhancing our understanding of intertidal ecosystem resilience, especially in the context of global change scenarios in which climate change-induced extreme weather events are becoming more frequent (Ummenhofer and Meehl 2017; AghaKouchak et al. 2020). Given the projected increase in extreme weather events, particularly storms, it is imperative to study the interplay between these extreme events and the daily sediment dynamics, as well as their impact on the macrofauna inhabiting tidal flats.

Our study aims to investigate the relationship between sediment dynamics and benthos composition, and how this relationship can affect the response of benthic communities to extreme weather events. Specifically, we want to understand how intensified sediment disturbances, caused by storms and other extreme weather events, can impact the abundance and mobility traits of macrofauna in intertidal mud flats. By examining how these organisms' mobility traits respond to varying levels of sediment dynamics, we hope to assess the resilience of tidal flat ecosystems to environmental changes and gain insights into the biogeomorphic processes that underpin their stability.

Studying the effects of climate change on sediment dynamics can be challenging as it often requires extended observation periods to capture natural changes or precise scheduling to accurately measure extreme events like storms. Therefore, an in situ experiment was conducted using plow rakes to simulate the physical disturbance in

sediments and increase sediment dynamics on tidal flats. Our hypothesis is that increased bed-level dynamics alter the benthic community structure by eliminating species with limited mobility traits. The experiment involved applying raking treatments six times biweekly at two Dutch tidal flats in the Scheldt estuary, covering a range of wind fetches that naturally occur in this system. Replicate raked and control plots were established at low and high elevations to compare areas across a range of inundation periods.

## Materials and methods

### Study sites

An in situ experiment was conducted on the Dutch tidal flats at Paulinapolder and Groot Buitenschoor, located along the coast of the Westerschelde estuary (Fig. 1a,b). The wave forcing and tidal level of each location were measured during the experimental period in 2019 using one pressure sensor (OSS1-010-003C; Ocean Sensor Systems) deployed 5 cm above the tidal flat surface of each site. The measurements were taken every 15 min, with a 7-min burst period during each measurement interval. The wave analysis was based on pressure fluctuations, measured with a frequency of 5 Hz. To measure the daily surface elevation dynamics (SED) with a high vertical and temporal resolution, one acoustic surface elevation dynamics (A-SED) sensor was deployed at each experimental site during a long-term campaign between 2019 and 2021 (see details about the acoustic surface elevation dynamics sensors in Willemsen et al. 2022). These sensors autonomously measure bed-level changes by capturing the echo of an acoustic signal, operating standalone without the need for external power or data-logging systems on tidal flats. Data collection consists of eight-sample bursts every 5 min, with the sensors oriented vertically toward the bottom. The collected data were then processed using a Python script to convert the acoustic signals into bed-level change information (Willemsen et al., 2022).

Numerous studies have used the terms “exposure” and “sheltered” to describe the wave and tide conditions experienced by various coastal areas (McLachlan 1980; Cardoso and Cabrini 2016). According to McLachlan et al. (2018), the Westerschelde estuary experimental zones are classified as tide-dominated flats, where wave heights typically do not exceed 0.5 m or are often calm. However, the two experimental locations at Paulinapolder and Groot Buitenschoor experience contrasting conditions of wind fetches, as shown in Supporting Information (Fig. S1). Hence, for the purposes of this study, we will use the terms “exposed” and “sheltered” to refer to the two experimental areas with varying wind fetches.

Although both sites belong to tide-dominated flats, Paulinapolder (referred to as *Sheltered*) is sheltered from the prevailing southwest wind direction, which results in limited waves compared to the water height; Groot Buitenschoor (referred to as *Exposed*) is more exposed to the prevailing wind conditions resulting in higher waves compared to the water

height (see Supporting Information Fig. S1). Considering the gradients in wave intensity over the tidal flat transect, the experiment was conducted at the low inundated salt marsh boundary ( $Exposed_{low}/Sheltered_{low}$ ; landward edge) and the high inundated seaward edge ( $Exposed_{high}/Sheltered_{high}$ ; channel-ward edge) of the two tidal flats (Fig. 1c,d). The elevations, tidal ranges, and emersion times of four different intertidal sites are shown in Table 1.

### Disturbing sediments by raking treatment

We used a plow rake alongside natural tidal currents to mimic the intensified sediment dynamics caused by storm events. This approach was adopted due to the inherent difficulties in assessing the impact of real storm events on benthic communities: (i) the widespread effects of storms on the entire ecotope complicate comparisons with unaffected communities; (ii) such fieldwork planning requires precise timing to effectively study these impacts. The rake had three tines, each with a width of 2 cm and a length of 9 cm. The tines collectively covered a total width of 15 cm, ensuring effective plowing of the experimental plots.

Given the local hydrodynamics and the daily elevation change of the deposit, we did not expect one or two instances of raking to result in significant changes in benthos composition in the experimental areas. Instead, we aimed to capture the cumulative impact over multiple events. Therefore, the raking disturbance was repeated six times every other week from March to June 2019 (Week 1 to Week 11, Fig. 1e). This period encompasses the typical recruitment period of macrobenthos. The repeated in situ raking had three primary purposes: first, to simulate the physical impacts of extreme weather events, such as storms, on intertidal deposits; second, to alter the sediment dynamics within the experimental areas, leading to increased topography changes; and third, to imitate the cumulative effect of sediment disturbance caused by the increasing frequency of storms under climate change, rather than a single disturbance event.

There were two raked plots and two control plots at each elevation of each tidal flat (see an example in Fig. 1f,g). Each experiment plot encompassed an area of  $2 \times 2$  m, with a central sampling area of  $1.5 \times 1.5$  m to minimize the edge effects during the sampling work. All plots were set parallel to the shoreline. Before the artificial disturbance, the microtopography was measured in each plot by setting up a 200-cm sedimentation erosion bar (SEB) at the corner of each raked plot (see details about sedimentation erosion bar in Nolte et al. 2013). The height between the sediment surface and the sedimentation erosion bar was measured every 10 cm across the plot before each raking treatment. After taking the sedimentation erosion bar measurements, the raking treatment was applied. The experiment plots were first raked parallelly and then perpendicularly to the shoreline to mimic a homogeneous physical disturbance on sediments (Fig. 1g). The raking depth was about 10 cm, the same as the plowing rake length.

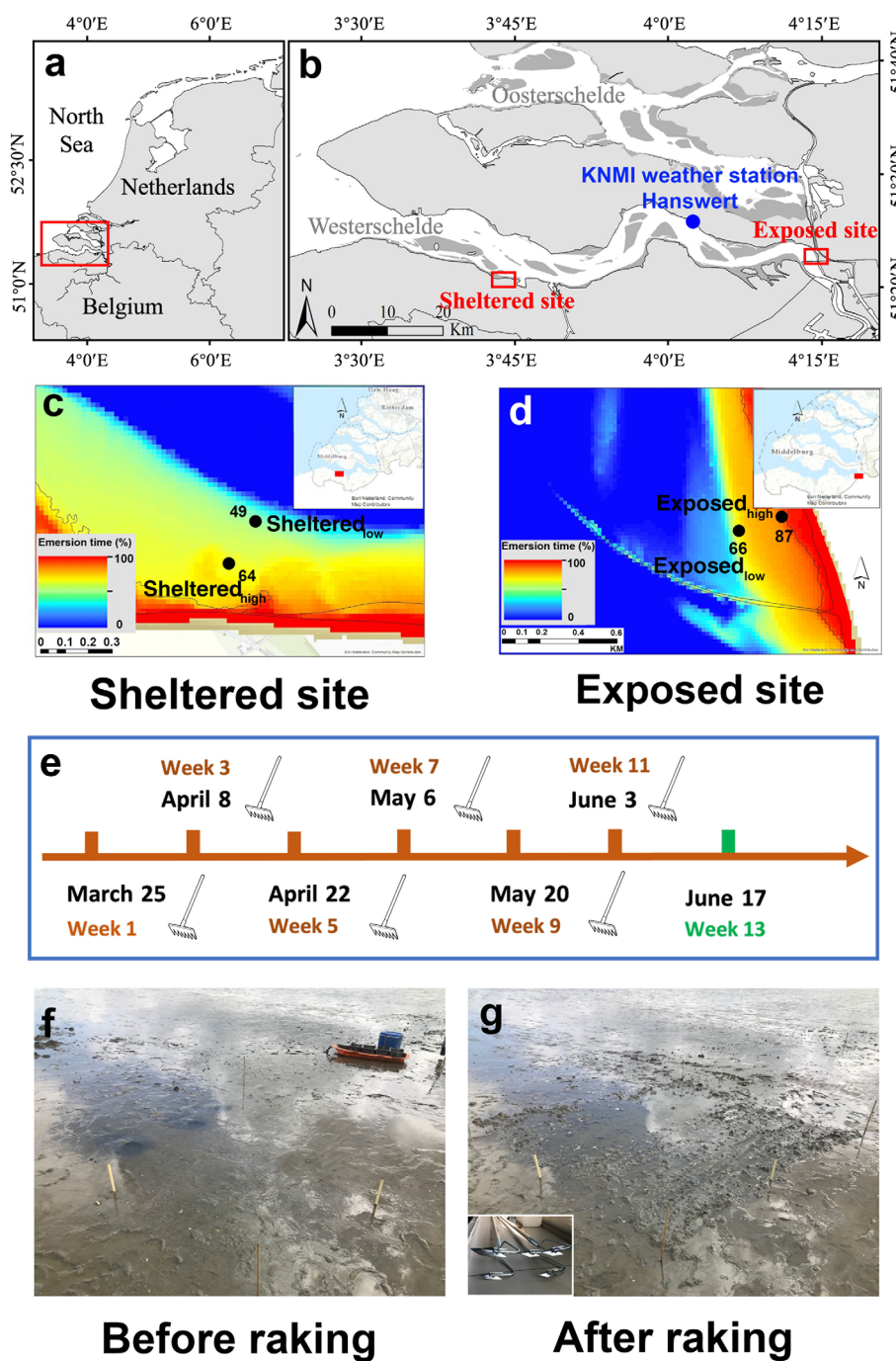


**Fig. 1.** Overview of experiment location and treatments. (a) The location of Western Scheldt in Western Europe; (b) the geographical distribution of the two chosen tidal flats and the Hanswert Royal Netherlands Meteorological Institute (KNMI) weather station in the Western Scheldt; (c, d) the emersion time of the wind-exposed and wind-sheltered sites, here 0% indicates permanent inundation while 100% indicates permanent emergence; (e) the experiment schedule for treatment and sampling work. The raking treatment was applied every 2 weeks from Week 1 to Week 11 (in total, six times, as indicated by the rake symbol); the green tick and labels refer to the sample harvest; (f, g) in situ photos of the same plot before and after the plow raking treatment at the Sheltered site, along with a picture showcasing the plow rake utilized in this experiment.

**Sampling biogeomorphic features**  
**Sediment samples**

Before each raking treatment, we collected four sediment samples in each plot using a 20-mL syringe, two for grain size

(3 cm height) and two for chlorophyll *a* (Chl *a*, 1 cm height) measurement. After collection in the field, sediment samples were stored in an icebox to preserve their integrity. Samples intended for Chl *a* measurements were immediately frozen



**Table 1.** The elevations, tidal ranges, and daily emersion time of four different sites. Two are located in a wind-sheltered area and two in a wind-exposed area. The values are expressed in relation to the Dutch ordnance level (NAP, the zero value being close to the mean sea level) and are presented as mean values and standard deviations. The tidal range of both Sheltered and Exposed locations is derived using data from Rijkswaterstaat, the Directorate-General for Public Works and Water Management. The daily emersion time is expressed as a percentage, with higher percentages indicating longer periods of time during which the site is in low tide and the sediments are exposed to air.

Sites	Location	Elevation (NAP, m)	Tidal range (NAP, m)	Daily emersion percentage
Sheltered <sub>low</sub>	Paulinapolder	-0.31 ± 0.02	-281 to 319	49
Sheltered <sub>high</sub>	Paulinapolder	0.74 ± 0.01		64
Exposed <sub>low</sub>	Groot Buitenschoor	1.11 ± 0.04	-317 to 378	66
Exposed <sub>high</sub>	Groot Buitenschoor	2.14 ± 0.01		87

at -80°C, while those designated for grain size measurement were stored at -20°C until further analysis. After acetone extraction, the Chl *a* content in sediments was measured using the Specord 210 spectrophotometer (Analytik Jena GmbH). To measure sediment grain size, the samples were placed in a freeze dryer for 72 h and then sieved through a 0.5-cm mesh to remove organisms and rocks. Then, the sediment grain size was measured using the Mastersizer 2000 analyzer (Malvern Panalytical Ltd.).

#### Macrobenthos and their biological traits

To monitor changes in macrobenthos communities between control and raked plots, samples were collected only at the end of the experiment to capture the cumulative effects of repeated raking disturbances (Fig. 1e). In each plot, three sediment cores were collected using 10-cm-diameter sampling cylinders to a depth of 30 cm. Sampling was conducted during low tide when the experimental areas were exposed, necessitating the transportation of sediment cores to the laboratory for processing, as in-field sieving was not feasible. The logistical challenges of handling and transporting large volumes of sediments, coupled with the labor-intensive nature of processing and identifying macrobenthos taxa, resulted in our decision to limit sampling to a single time point at the end of the experiment.

Based on the study conducted by Celentano et al. (2019), the vertical distribution of macrobenthos species on tidal flats follows a pattern where the upper strata, which include depths of 0–5 and 5–10 cm, have a significantly higher richness and density than depths greater than 15 cm. Another study by Ysebaert and Herman (2002) quantified the distribution and abundance of benthic macrofauna in the Westerschelde estuary. Their results showed that macrobenthic communities are dominated by a few species, mainly surface deposit feeders like *Corophium volutator* and sub-surface deposit feeders like *Heteromastus filiformis*. *Corophium volutator* usually reworks the top 3 cm of sediments and exerts bioturbation effects through their burrowing behaviors, while *H. filiformis* usually digs and makes their feeding tubes under the sediment surface at 10–30 cm.

Each sampling cylinder was sliced into three pieces along a depth gradient to study the impact of raking treatment on

macrobenthos, considering the distribution and mobility traits of the historically dominant species in the experimental areas. The three depths are 0–5, 6–10, and 11–30 cm, corresponding to the upper active layer, lower active layer, and inactive layer, respectively. The upper active layer is easily disturbed in natural conditions, even without raking. The lower active layer is rarely disturbed, except by raking or extreme events. The inactive layer is never disturbed under natural conditions or the raking treatment.

The macrobenthos were sieved from the sediments using a 1.0-mm mesh sieve, allowing smaller particles and organisms to pass through while retaining the target macrobenthic species (Ysebaert and Herman 2002). Specimens that did not exhibit benthic living styles or were undeveloped larvae were eliminated based on expert opinions from co-authors. All specimens were identified at the lowest taxonomic level and subsequently classified into different mobility traits according to a classification table by Queirós et al. (2013). Mobility scores ( $M_i$ ) were given to each species. “1” represents organisms that live in fixed tubes; “2” indicates organisms with limited movement; “3” indicates organisms with slow, free movement through the sediment matrix; while “4” indicates organisms with free movement via a burrow system (Queiros et al., 2013). After counting the abundance, the benthic animals were dried for 48 h at 80°C and then burned in a muffle oven (510°C) for 3 h to measure the ash-free dry weights (AFDW). Species’ mobility traits and their corresponding presence are provided in Table 2. We consulted with experts in the field to determine these values (Beauchard et al. 2022).

#### Critical erosion thresholds

At the conclusion of the experiment, five sediment cores were collected from each plot to measure the critical erosion threshold of the tidal flat using the Oscillatory-Channel Resuspension flume (the OsCaR-flume), which simulates the near-bed hydrodynamics of waves (de Smit et al., 2021). The OsCaR-flume is specifically designed for assessing the erodibility of natural sediments without aboveground benthic structures (de Smit et al., 2021). It is based on oscillatory flow tunnels (also known as U-tubes), which are used to study

**Table 2.** A summary of macrobenthos species presence in respective experimental sites. Mobility scores ( $M_i$ ) were listed as, “1” for organisms that live in fixed tubes; “2” indicates limited movement; “3” indicates slow, free movement through the sediment matrix; “4” indicates free movement via burrow system.

Species	Class	$M_i$	Exposed <sub>low</sub>	Exposed <sub>high</sub>	Sheltered <sub>low</sub>	Sheltered <sub>high</sub>
<i>Abra alba</i>	Bivalvia	2		+		+
<i>Abra tenuis</i>	Bivalvia	2			+	
<i>Alitta succinea</i>	Polychaeta	4	+	+	+	+
<i>Brachyura</i> sp.	Malacostraca	4			+	+
<i>Capitella</i> sp.	Polychaeta	2		+		+
<i>Carcinus maenas</i>	Malacostraca	4			+	+
<i>Cardiidae</i> sp.	Bivalvia	2				+
<i>Cerastoderma edule</i>	Bivalvia	2			+	+
<i>Cirratulidae</i> sp.	Polychaeta	2			+	
<i>Corophium</i> sp.	Malacostraca	4	+	+	+	
<i>Crab</i> juvenile	Malacostraca	4			+	+
<i>Crangonidae</i> sp.	Malacostraca	4			+	+
<i>Cyathura carinata</i>	Malacostraca	2	+	+	+	+
<i>Eteone</i> sp.	Polychaeta	3			+	+
<i>Hediste diversicolor</i>	Polychaeta	4	+	+	+	
<i>Heteromastus filiformis</i>	Polychaeta	2	+	+	+	+
<i>Lanice conchilega</i>	Polychaeta	1			+	
<i>Limecola balthica</i>	Bivalvia	2	+	+	+	+
<i>Modiolula phaseolina</i>	Bivalvia	2			+	
<i>Nereididae</i> sp.	Polychaeta	4		+	+	+
<i>Oligochaeta</i> sp.	Oligochaeta	3	+	+	+	+
<i>Peringia ulvae</i>	Gastropoda	3				+
<i>Phyllodoce mucosa</i>	Polychaeta	3			+	
<i>Retusa obtusa</i>	Gastropoda	3				+
<i>Ruditapes philippinarum</i>	Bivalvia	2				+
<i>Sabellida</i> sp.	Polychaeta	1		+		
<i>Scrobicularia</i> sp.	Bivalvia	2	+		+	+
<i>Spionidae</i> sp.	Polychaeta	1			+	
<i>Tellinoidea</i> sp.	Bivalvia	2		+		+

sediment dynamics and near-bed hydrodynamics under full-scale ocean waves (O’Donoghue and Clubb 2001; Ribberink et al. 2008). These tunnels replicate wave boundary layer conditions, where the vertical velocity component of waves diminishes toward the seabed, resulting in oscillatory water motion at the bed (Jonsson and Carlsen 1976). By imposing the representative oscillatory velocity and orbital excursion length, the near-bed hydrodynamics of storm waves can be generated. The erosion threshold was measured by gradually increasing the oscillatory velocity until the sediment resuspension rate exceeded a critical value of  $0.06 \text{ g m}^{-2} \text{ s}^{-1}$ , corresponding to the bed erosion (see details in de Smit et al., 2021).

## Data analysis

### Sediment dynamics and topography change

We used the method described by Grandjean et al. (2023) to obtain morphodynamic signature indices from daily surface elevation dynamics time series data, which

were utilized to describe the typical local sediment dynamics. We calculated the return time of the daily bed-level dynamics at each site, which indicates the frequency at which specific bed-level changes are likely to occur. Furthermore, the autocorrelation function (ACF) was applied to calculate the correlation length of the elevation change. These autocorrelation lengths are used to demonstrate the long-term persistence of surface elevation over time and reflect the duration at which environmental conditions change for organisms, serving as an indicator of the extent to which species can withstand environmental fluctuations (van Belzen et al. 2022). A higher value of the autocorrelation length indicates that the physical environment (i.e., the bed level) takes a longer time to change and is, hence, more suitable for organisms at that location (Grandjean et al., 2023). Return time is a proxy for the short-term bed-level changes whereas autocorrelation length values can indicate the long-term bed-level evolution.

### Species mobility traits and sediment dynamics

The abundance data standardized to area was summarized based on sampling depth and species mobility traits in order to examine the impact of frequent physical disturbances on species abundance across various mobility traits. This dataset did not pass the Shapiro test for normality after log transformation; therefore, an unpaired Wilcoxon test was used for statistical analysis. The total species abundance of each mobility trait was summarized according to the corresponding correlation length at each experimental site, to display the relationship between sediment dynamics and trait-based species abundance.

### Macrofauna abundance and community structure

Community structure was investigated by means of principal component analysis on instrumental variables (PCAIV; Lebreton et al. 1991). In our context, the experimental treatments were categorical variables that were used to deconstruct the multi-dimensional variance of the *samples* × *taxa* contingency table into single, additive, and interactive parts. The contingency table was preliminarily processed by correspondence analyses (CA), leading to canonical correspondence analysis (CCA; ter Braak 1986) as a particular case of principal component analysis on instrumental variables (Thioulouse et al. 2018). Analyses were performed on individual densities, and principal component analysis on instrumental variables interpretations were applied to the pattern yielding the highest explained correspondence analyses variance by the three-factor additional effect. Variance significances were tested by a permutation procedure of the explanatory matrix rows (Thioulouse et al. 2018). The use of correspondence analyses was justified by the search for a relationship between environment factors (*samples*) and organism mobility traits (*taxa*) through species correspondences. To examine this relationship, we employed the Fourth corner method (Dray et al. 2014), which confronted the axes (representing sample positions) of principal component analysis on instrumental variables with the species-defined traits (Fig. 2).

All analyses were performed in R 4.3.1 (R Core Team 2023) with the package *ade4* (Chessel et al. 2004; Dray et al. 2007).

## Results

### Topographic response to frequent sediment disturbance

The Exposed<sub>high</sub> site experienced the most sudden changes in surface elevation, as indicated by the lowest autocorrelation length of 29 d. In contrast, the Sheltered<sub>high</sub> site was the most stable in the long term, with the longest autocorrelation length of 122 d. The Exposed<sub>low</sub> and Sheltered<sub>low</sub> sites exhibited distinct autocorrelation lengths, with durations of 36 and 55 d, respectively (see details in Supporting Information Fig. S2). In terms of short-term bed-level dynamics, the return time analysis revealed overlapping patterns between the Sheltered and Exposed sites. The Sheltered sites exhibited relatively longer return times, ranging from 1.44 d mm<sup>-1</sup> (Sheltered<sub>high</sub>) to 6.36 d mm<sup>-1</sup> (Sheltered<sub>low</sub>). On the other hand, the Exposed

sites experienced shorter return times, ranging from 1.32 d mm<sup>-1</sup> (Exposed<sub>low</sub>) to 1.59 d mm<sup>-1</sup> (Exposed<sub>high</sub>). The average return time under specific daily elevation changes is displayed in Supporting Information Fig. S2.

The repeated physical disturbances by raking resulted in significant sediment erosion at all experimental plots (Fig. 3a). The raking treatment significantly increased the daily erosion depth with larger impacts at the Exposed sites compared to the Sheltered sites (see Fig. 3a the red dashed line is a reference of no elevation change at 0 mm 14 d<sup>-1</sup>; the results of Wilcoxon test are shown in Table 3). Most erosion occurred within the first three raking treatments, except for the site Sheltered<sub>high</sub>, which was more resistant in the beginning. The site Exposed<sub>low</sub> experienced the largest erosion, up to 2.5 cm. The time-series changes in elevation, as measured by sediment erosion bars, are presented in Supporting Information Fig. S3.

The mean sediment grain size was measured in both Sheltered and Exposed areas. In the Sheltered area, the low inundated site had a median grain size  $D_{50}$  of  $86.47 \pm 8.25 \mu\text{m}$ , while the high inundated site had a mean  $D_{50}$  of  $69.29 \pm 6.80 \mu\text{m}$ . These values classify the sediment as very fine sand (63–125  $\mu\text{m}$ ) according to the categories listed by Blott and Pye (2001). In contrast, in the Exposed area, the low inundated site had a mean grain size  $D_{50}$  of  $50.15 \pm 5.07 \mu\text{m}$ , and the high inundated site had a mean  $D_{50}$  of  $47.39 \pm 3.97 \mu\text{m}$ . The sediments in the Exposed area fell within the range of very coarse silt (31–63  $\mu\text{m}$ ) according to the same classification system.

The critical erosion threshold ( $U_{\text{max}}$ ) measured with the OsCaR-flume showed only a significant difference between the raked and control plots for Exposed<sub>high</sub> (Fig. 3b,  $W = 52$ ,  $N = 8$ ,  $p = 0.007$ ). The Chl *a* content and grain size within the surface sediment layer did not experience significant change after the raking treatment (Supporting Information Fig. S4). Except the Chl *a* content decreased with increasing times of raking treatments at Exposed<sub>low</sub>.

### Community structures of macrofauna in Exposed and Sheltered sites

A total of 29 macrobenthos taxa were captured in the experimental intertidal areas (Table 2). The Sheltered site had a total of 27 taxa, while the Exposed sites had a smaller community of 13 taxa. Among the taxonomic groups, Polychaeta and Mollusca emerged as the most abundant groups, each comprising 11 taxa. Crustacea showcased a notable presence with five taxa, and Oligochaeta displayed the least representation, with only one taxa detected.

The principal component analysis on instrumental variables was performed to investigate the relationships between species composition, raking treatments, site characteristics, and sediment depths (Fig. 2). The community pattern resulting from the combination of the other three factors was expressed along two main axes (Fig. 2a). Axis 1, accounting for the main variation, separated the two sites (see Fig. 2c). The positive (right) section of the 1<sup>st</sup> axis is associated with species predominantly





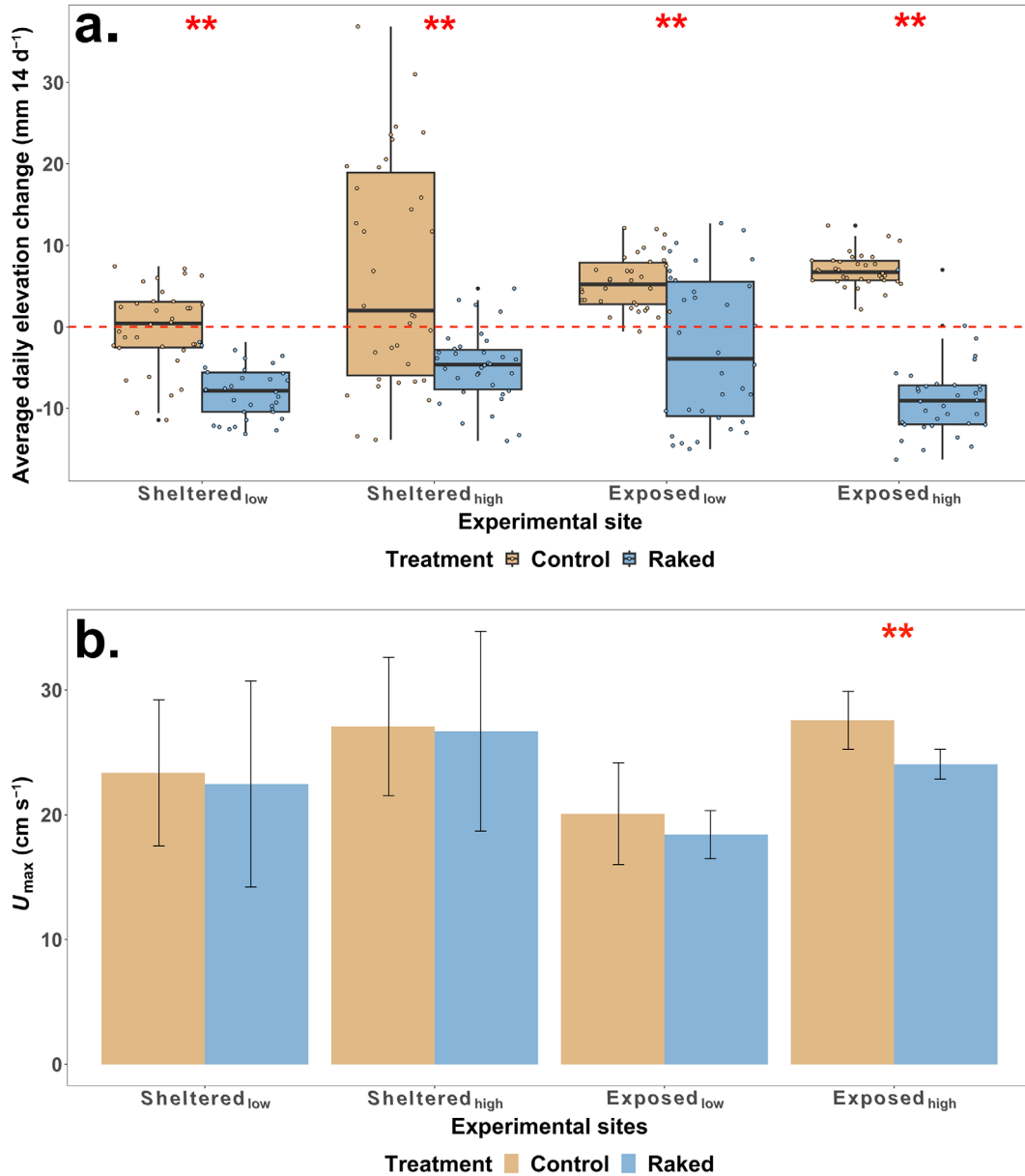


**Fig. 3.** Sediment stability during the experimental periods. **(a)** The average daily bed-level change between control and raked plots measured by sediment erosion bars. The average daily change of bed-level was calculated by the biweekly measurements divided by 14 (days of 2 weeks). Each box plot contains 34 data points. The red dashed line shows no elevation change at 0 mm 14 d<sup>-1</sup>. **(b)** A summary of critical erosion thresholds measured by the OsCaR-flume measurements.  $U_{\max}$  is the maximum current speed that induces erosion of the cohesive sediment underneath. Each bar represents the mean value derived from 5 to 9 data points. The difference between control and raked plots was examined using the Wilcoxon test. The statistical significance at the  $p < 0.01$  level was denoted by “\*\*.”

found in Sheltered sites, notably dominated by *Heteromastus filiformis* (across all plots, mean abundance:  $1412 \pm 728$  ind. m<sup>-2</sup>, mean ash-free dry weights =  $22.95 \pm 21.20$  g m<sup>-2</sup>), while the negative (left) part of the 1<sup>st</sup> axis corresponds to species mainly observed in Exposed sites, with *Corophium* sp. as the dominant species (across all plots, mean abundance:  $8392 \pm 5872$  ind. m<sup>-2</sup>, mean ash-free dry weights =  $45.56 \pm 22.39$  g m<sup>-2</sup>). Axis 2 mainly expressed variations between sediment depths (see Fig. 2d). The negative (bottom) section of the 2<sup>nd</sup> axis represents

species primarily found at shallower depths, specifically within the range of 0–5 cm. In contrast, the positive (top) section of the 2<sup>nd</sup> axis indicates species inhabiting depths ranging from 5 to 30 cm.

In general, the community structure was significantly affected by the joint effects of raking treatments, site characteristics, and sediment depths, and these three factors explained 30.6% of the total multidimensional variance (referred to as “explained inertia”) with a  $p$ -value < 0.01.

Among these, no raking effect on community structure was found (Fig. 2b, explained inertia: 1.2,  $p = 0.83$ ), whereas site characteristics (explained inertia: 17.1,  $p < 0.01$ ) and sediment depths (explained inertia: 12.0,  $p < 0.01$ ) had substantial effects. Although the upper sediment layer (0–5 cm) was more distant from the deeper ones (6–10 and 11–30 cm) in both

sites (Fig. 2d), the upper layer from the sheltered site hosted the taxa with the smallest niche breadths such as *Cerastoderma edule*, *Eteone* sp., *Modiolula phaseolina*, *Retusa obtusata*, and *Ruditapes philippinarum* (Fig. 2f). The Fourth corner analysis reveals that the environmental variables (i.e., raking treatments, site characteristics, and sediment depths) did not change the organism mobility traits ( $p > 0.05$ ).

**Table 3.** Wilcoxon rank-sum test results for mean daily bed-level change. The  $N$  represents the number of observations for each group. The  $W$  indicates the Wilcoxon rank-sum statistic, which is used to evaluate the sum of ranks for one of the groups being compared. The  $p$ -values indicate the statistical significance of differences between control and raked plots, with “\*\*\*\*” denoting  $p < 0.01$ .

	Sheltered		Exposed	
	Low	High	Low	High
$N$	34	34	34	34
$W$	1031	851.5	851.5	1137
$p$ -value	<0.001**	0.00081**	0.00081**	<0.001**

**Species traits under frequent sediment disturbance**

Species trait analysis revealed that free-moving mobile species (e.g., *Co. volutator*) contributed most of the macrofauna abundance at the Exposed sites. In contrast, species with limited- or slow-moving ability (immobile) shared most proportions of the macrofauna at the Sheltered sites (Fig. 4). Specifically, high-mobility species ( $M_i = 4$ ) showed higher abundance at both Exposed<sub>low</sub> and Exposed<sub>high</sub> with lower correlation lengths (i.e., more dynamic areas). In comparison, low-mobility species ( $M_i = 2$ ) showed higher abundance at both Sheltered<sub>low</sub> and Sheltered<sub>high</sub> with higher correlation lengths (i.e., slowly changing areas).

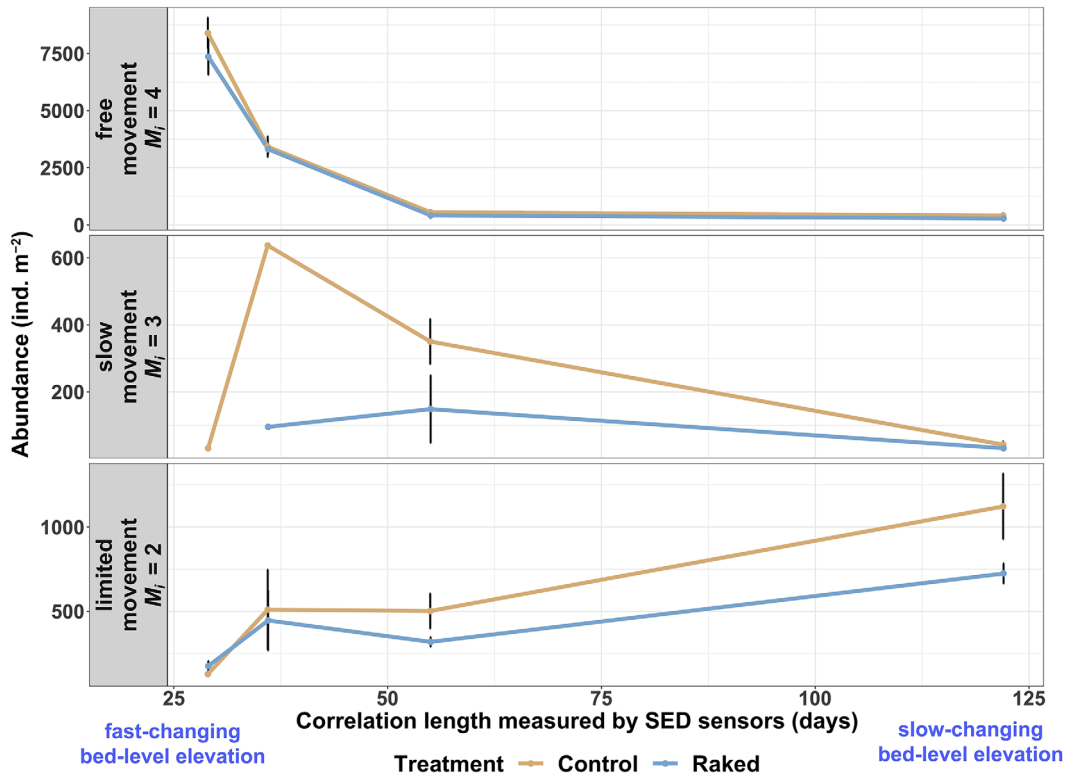


**Fig. 4.** The relationship between the correlation length and the species abundance as categorized by mobility traits. Low correlation length values indicate a fast-changing bed-level elevation and strong sediment dynamics, while high correlation length values indicate a slow-changing bed-level elevation and weak sediment dynamics. “ $M_i$ ” represents the mobility index score (species mobility increases from 1 to 4, “1” for organisms that live in fixed tubes; “2” indicates limited movement; “3” indicates slow, free movement through the sediment matrix; “4” indicates free movement via burrow system); the mobility score 1 was not shown because no samples belonged to this category. Each point represents 3–5 data recordings in (a) and (c), and 1–4 recordings in (b), depending on the species trait presence. The error bars represent the standard errors between replicate cores; the error bar was not shown if only one data point existed.

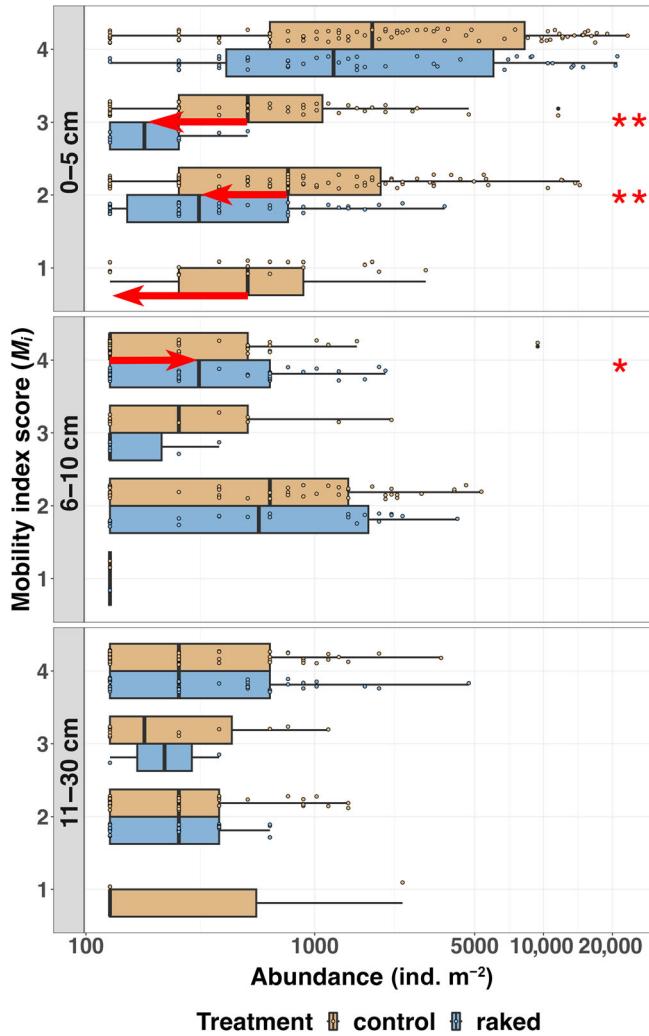


**Fig. 5.** Effects of raking treatments on species abundance with different mobility traits. The facet name indicates the sampling depth below the sediment surface. The x-axis indicates the log-transformed species abundance. The y-axis in each facet shows the mobility trait as indicated by the mobility index score (species mobility increases from 1 to 4, “1” for organisms that live in fixed tubes; “2” indicates limited movement; “3” indicates slow, free movement through the sediment matrix; “4” indicates free movement via burrow system). The red arrows indicate significant changing trends of trait-based abundance in respective depths. The difference between control and raked plots is tested using the Wilcoxon test. The significant level of  $p < 0.05$  was indicated by “\*.” The significant level of  $p < 0.01$  was indicated by “\*\*.”

The total abundance of macrofauna in the surface 0–5 cm sediments decreased in a trait-specific way after repeating raking six times (Fig. 5). The six-time repeated raking treatments significantly reduced the abundance of low-mobility species in 0–5 cm sediments ( $M_i = 2$  and 3,  $F_{M_i=2} = 2378.5$ ,  $p_{M_i=2} = 0.0078$ ,  $F_{M_i=3} = 356.5$ ,  $p_{M_i=3} = 0.00999$ ). The high-mobility species significantly increased in the 6–10 cm sediments ( $F_{M_i=4} = 568.5$ ,  $p_{M_i=4} = 0.016$ ), though they did not experience a significant change in the top 5 cm depth (Fig. 5).

## Discussion

An in-depth understanding of community resilience is important to predict the ecosystem resilience to future climate change, especially as tidal velocities and more frequent storms are expected to influence the daily bed-level dynamics. In the current experiment, we increased the physical disturbance to mimic enhanced sediment dynamics by a raking treatment. The Exposed<sub>high</sub> site exhibited a significant topographical reduction of up to 2.5 cm following six repeated physical disturbances after 12 weeks. This was evidenced by an extended return period for bed-level alterations and a diminished autocorrelation length. In contrast, the Sheltered<sub>high</sub> site hardly eroded in the beginning, as indicated by the low return time of bed-level changes and high autocorrelation length (see Supporting Information Fig. S2). The traits of the macrobenthic community are intricately connected to the internal environmental variability of the location they inhabit: locations characterized by frequent high-magnitude changes in bed-level tend to exhibit a greater abundance of species with high mobility.

Overall, the benthic macrofauna showed consistent species composition despite the enhanced sediment disturbance event, and the highly mobile species responded by burrowing deeper into the sediments. However, the abundance of certain immobile bivalve and polychaete species might experience declines. This implies that the macrofauna can still support similar species on higher trophic levels. The reduced food availability and energy flow due to lower macrofauna numbers can affect the population dynamics and sustainability of higher trophic levels, such as birds and fishes, thereby influencing the broader ecosystem services and functioning these organisms provide.

## Sediment dynamics as tools to monitor ecological stability

The present study reveals that both short-term and long-term sediment dynamics are essential tools for monitoring the internal environmental variance and ecological stability of tidal flats. Previous studies identified many other factors that may indicate the stability of the tidal flat ecosystems, such as the critical erosion thresholds (Bale et al. 2006; de Smit et al. 2021), Chl *a* (Morys et al. 2016), and sediment grain size (Garwood et al. 2015; van der Wal et al. 2017), though these factors did not show an overall significant difference between raked and control plots after six raking treatments in 12 weeks. However, significant bed-level erosion was observed at all locations after six raking-recovery cycles (Fig. 3a). Moreover, the raking treatments significantly affected the macrofauna abundance: species with limited mobility were removed from the surface layer of 0–5 cm sediments, while mobile species burrowed deeper into 5–10 cm sediments (Fig. 5).

Most benthic organisms inhabit in the top 10 cm of sediments, making them vulnerable to disturbance at the sediment–water interface (Poole and Stewart 1976; Weston 1990). Several

studies also indicate that the effects of storms on tidal flat species depend on their mobility traits (Pagès et al. 2013). For example, the low-mobility bivalve *Meretrix meretrix* ( $M_i = 2$ ) was dislodged up to 50% of their density and biomass during extreme physical disturbance caused by storms (Shi et al. 2021). However, highly mobile species, such as the fish *Sarpa salpa*, can escape from the storm disturbance (Pagès et al. 2013). Therefore, benthic species inhabiting areas with reduced bed-level dynamics (i.e., higher autocorrelation length values) are generally more susceptible to physical disturbances. These disturbances may potentially modify the abundance and composition of macrofauna on tidal flats, favoring mobile species with smaller body sizes. As a result, such homogenization of species traits can have cascading effects on energy flow within food webs. In general, the reduction in abundance and body size may decrease food source availability for higher trophic levels, such as birds that rely on larger prey like shellfish and large worms (Jennings and Kaiser 1998; Mueter et al. 2021). This, in turn, can alter the feeding patterns and population dynamics of birds on tidal flats (Meire et al. 1994; Lewis et al. 2003). Additionally, changes in the macrobenthic abundance of bioturbating species may influence nutrient cycling in depositional environments (Braeckman et al. 2010). For example, the high density (6000 ind. m<sup>-2</sup>) of the amphipod crustacean *Co. volutator* increased the nitrogen removal up to 1.5-fold via burrowing activities compared with sediments with no *Co. volutator* (Pelegri and Blackburn 1994).

Furthermore, the elevation change resulting from the raking experiment does not surpass the natural bed-level fluctuations observed across all locations (see Supporting Information Fig. S2). Nevertheless, the Exposed<sub>high</sub> site exhibited more pronounced bed-level changes during 1 yr of measurements conducted by the acoustic surface elevation dynamics sensors, displaying an approximate variance of 8 cm. This increase in variance is likely attributed to nonconsolidated sediments, which are more susceptible to erosion. Notably, during the OsCaR-flume experiment, we only observed a divergence in the critical erosion threshold between the raked and control plots at this specific site (refer to Fig. 3b). The sedimentation erosion bar results show that the raked plots suffered more vigorous long-term erosion than the nonraked treatments; this more substantial erosion removed the raking-loosened mud from the surface of tidal flats, resulting in sediments with higher critical shear stress. Therefore, we speculate that the effects of physical (raking) disturbance depend on the natural tidal flat dynamics and the consolidation of the top layer sediment. Constant raking treatment leads to erosion, however, the ability to recover from critical erosion thresholds varies depending on the natural sediment dynamics in each area. If the (raking) disturbance depth is within the natural elevation variance, we expect that the surface (0–5 cm) sediment can quickly recover to predisturbance characteristics; otherwise, there will be a significant difference in the critical erosion thresholds.

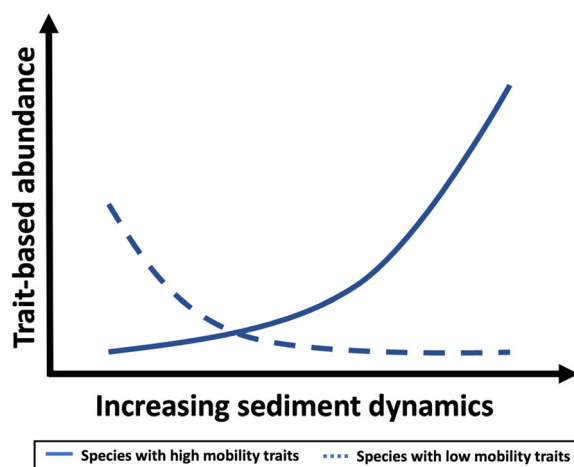


**Fig. 6.** A conceptual figure illustrating the filtering effects of sediment dynamics on species' biological traits. Solid lines indicate species possessing specific biological traits that aid in their resilience to the increasing sediment dynamics, while dashed lines represent less-tolerant species in response to the sediment dynamics. Notably, as the abundance of species with high mobility traits rises, the community resilience to enhanced sediment dynamics may also increase.

### Translating environmental variance into community resilience

External disturbance plays an important role in shaping the community assembly, though the community experiences natural dynamics in species abundance due to intrinsic relationships such as competition and predation (Turner 2010). Species that cannot withstand the predominant disturbance regime will be filtered out so that the remaining community will gradually adapt to prevailing environmental conditions due to the filtering for specific living styles (Diaz et al. 1998). As such, ecosystems have “memories” in that the experience of environmental conditions may influence the present community structure, thus defining their resilience to future environmental change (Johnstone et al. 2016).

Ecosystem resilience usually refers to the capacity to undertake disturbance yet not permanently lose the key ecological structures and functions (O'Brien et al. 2018). Extreme weather events, such as extreme storms and floods, are usually stochastic external disturbance that surpasses the ecosystem memory (Johnstone et al. 2016; Turner et al. 2020). The present in situ experiment reveals the relationship between internal environmental variance and community resilience to external disturbance: (i) increasing sediment dynamics filter species with high mobility traits in time, while species with low mobility traits decrease in abundance (Fig. 6, based on results in Fig. 4); (ii) community resilience to sediment dynamics may correlate positively with the dominant mobility trait, which is an essential part of the ecosystem memories (based on Fig. 5). The autocorrelation length value indicates how quickly environmental conditions change for organisms that need to cope with

environmental fluctuations (van Belzen et al. 2022; Grandjean et al. 2023). The Exposed sites, characterized by lower autocorrelation length values (i.e., faster-repeating changes in the bed-level evolution), are dominated by more mobile species such as *Corophium* sp. (see Table 2). In contrast, the Sheltered tidal flats with high autocorrelation length values (i.e., slowly changing bed-levels) are dominated by less active species, such as shellfish and worms (Table 2). The raking treatment was applied multiple times, coinciding with the spat season (from March to June). Unfortunately, due to the limitation of a one-time harvest of macrobenthos samples, we were unable to conduct a more detailed analysis comparing the effects of multiple raking treatments on sediment disturbance. Future studies could benefit from employing finer sampling techniques to capture the responses of different life stages across a broader range of species, enabling a more comprehensive understanding of the resilience and adaptability of macrobenthic communities to varying levels of disturbance (Bremner et al. 2006; Fu et al. 2022). Nevertheless, our observations comparing control and raked plots revealed that mobile species managed to recolonize disturbed areas despite recurrent raking events. In contrast, species with low mobility were unable to recover within the bi-weekly intervals of disturbance, suggesting a potential resilience threshold associated with mobility.

The present study highlights the potential of decreasing ecosystem productivity and resilience under climate-change-induced extreme weather events and tidal amplitude increase, with the exact impact depending on ecosystem memories shaped by species' biological traits (Bernhardt and Leslie 2013; Gravina et al. 2020). Therefore, regular monitoring of the environmental conditions will provide essential knowledge to predict the spatial and temporal vulnerability of ecosystem functioning and help lower the risks of biodiversity loss.

### Conclusions and outlook

Extreme weather events can significantly affect biodiversity and ecosystem functioning (Ummenhofer and Meehl 2017). As global warming continues, storms are likely to become more frequent and intense, exacerbating this impact (Bevacqua et al. 2019). Our experiment has shown that tidal flats with limited sediment dynamics are more susceptible to abundance loss compared to those with high sediment dynamics. Due to the environmental filtering effects under projected changes, we may expect that: (i) macrofauna in low sediment dynamic tidal flats may shift toward more mobile species, despite being already vulnerable to disturbances; (ii) macrofauna in more dynamic areas are expected to be able to cope with more frequent disturbances, as long as the disturbances remain within the range they can cope with.

Furthermore, our study suggests that the biogeomorphic system of tidal flats with high sediment dynamics and mobile

macrofauna are resilient to increased sediment disturbances. In contrast, systems with limited sediment dynamics and less mobile macrofauna are highly impacted and will likely shift toward hosting more mobile species in their benthic community. By the regulation of sediment dynamics, a favorable deposit environment can be created to enhance the establishment and survival of less-mobile benthic macrofauna, potentially leading to substantial benefits for higher trophic levels, including migratory bird populations. Overall, our research highlights the importance of understanding how biogeomorphic features respond to climate change scenarios to effectively manage valuable tidal flat ecosystems.

### Data availability statement

The data that support the findings of this study are available from the corresponding author upon reasonable request.

### References

- AghaKouchak, A., and others. 2020. Climate extremes and compound hazards in a warming world. *Annu. Rev. Earth Planet. Sci.* **48**: 519–548. doi:10.1146/annurev-earth-071719-055228
- Bale, A. J., J. Widdows, C. B. Harris, and J. A. Stephens. 2006. Measurements of the critical erosion threshold of surface sediments along the Tamar Estuary using a mini-annular flume. *Cont. Shelf Res.* **26**: 1206–1216. doi:10.1016/j.csr.2006.04.003
- Beauchard, O., S. Mestdagh, L. Koop, T. Ysebaert, and P. Herman. 2022. Benthic synecology in a soft sediment shelf: Habitat contrasts and assembly rules of life strategies. *Mar. Ecol. Prog. Ser.* **682**: 31–50. doi:10.3354/meps13928
- Bernhardt, J. R., and H. M. Leslie. 2013. Resilience to climate change in coastal marine ecosystems. *Ann. Rev. Mar. Sci.* **5**: 371–392. doi:10.1146/annurev-marine-121211-172411
- Bevacqua, E., D. Maraun, M. I. Voudoukas, E. Voukouvalas, M. Vrac, L. Mentaschi, and M. Widmann. 2019. Higher probability of compound flooding from precipitation and storm surge in Europe under anthropogenic climate change. *Sci. Adv.* **5**: eaaw5531. doi:10.1126/sciadv.aaw5531
- Blott, S. J., and K. Pye. 2001. GRADISTAT: A grain size distribution and statistics package for the analysis of unconsolidated sediments. *Earth Surf. Process. Landf.* **26**: 1237–1248. doi:10.1002/esp.261
- Borsje, B. W., T. J. Bouma, M. Rabaut, P. M. J. Herman, and S. J. M. H. Hulscher. 2014. Formation and erosion of biogeomorphological structures: A model study on the tube-building polychaete *Lanice conchilega*. *Limnol. Oceanogr.* **59**: 1297–1309. doi:10.4319/lo.2014.59.4.1297
- Bouma, H., J. M. C. Duiker, P. P. de Vries, P. M. J. Herman, and W. J. Wolff. 2001. Spatial pattern of early recruitment of *Macoma balthica* (L.) and *Cerastoderma edule* (L.) in



- relation to sediment dynamics on a highly dynamic intertidal sandflat. *J. Sea Res.* **45**: 79–93.
- Braeckman, U., P. Provoost, B. Gribsholt, D. Van Gansbeke, J. Middelburg, K. Soetaert, M. Vincx, and J. Vanaverbeke. 2010. Role of macrofauna functional traits and density in biogeochemical fluxes and bioturbation. *Mar. Ecol. Prog. Ser.* **399**: 173–186. doi:[10.3354/meps08336](https://doi.org/10.3354/meps08336)
- Bremner, J., S. Rogers, and C. Frid. 2006. Methods for describing ecological functioning of marine benthic assemblages using biological traits analysis (BTA). *Ecol. Indic.* **6**: 609–622. doi:[10.1016/j.ecolind.2005.08.026](https://doi.org/10.1016/j.ecolind.2005.08.026)
- Cardoso, R. S., and T. M. Cabrini. 2016. Population dynamics and secondary production of gastropods on a sheltered beach in south-eastern Brazil: A comparison between an herbivore and a scavenger. *Mar. Freshw. Res.* **68**: 87–94.
- Cazenave, A., and G. L. Cozannet. 2014. Sea level rise and its coastal impacts. *Earth's Future* **2**: 15–34. doi:[10.1002/2013EF000188](https://doi.org/10.1002/2013EF000188)
- Celentano, E., D. Lercari, P. Maneiro, P. Rodríguez, I. Gianelli, L. Ortega, L. Orlando, and O. Defeo. 2019. The forgotten dimension in sandy beach ecology: Vertical distribution of the macrofauna and its environment. *Estuar. Coast. Shelf Sci.* **217**: 165–172. doi:[10.1016/j.ecss.2018.11.008](https://doi.org/10.1016/j.ecss.2018.11.008)
- Chessel, D., A. B. Dufour, and J. Thioulouse. 2004. The ade4 package-I-one-table methods. *R News* **4**: 5–10.
- de Smit, J. C., M. Z. M. Brückner, K. I. Mesdag, M. G. Kleinhans, and T. J. Bouma. 2021. Key bioturbator species within benthic communities determine sediment resuspension thresholds. *Front. Mar. Sci.* **8**: 726238. doi:[10.3389/fmars.2021.726238](https://doi.org/10.3389/fmars.2021.726238)
- de Vet, P. L. M., B. C. van Prooijen, I. Colosimo, N. Steiner, T. Ysebaert, P. M. J. Herman, and Z. B. Wang. 2020. Variations in storm-induced bed level dynamics across intertidal flats. *Sci. Rep.* **10**: 12877. doi:[10.1038/s41598-020-69444-7](https://doi.org/10.1038/s41598-020-69444-7)
- Diaz, S., M. Cabido, and F. Casanoves. 1998. Plant functional traits and environmental filters at a regional scale. *J. Veg. Sci.* **9**: 113–122. doi:[10.2307/3237229](https://doi.org/10.2307/3237229)
- Dray, S., A. B. Dufour, and D. Chessel. 2007. The ade4 package-II: Two-table and K-table methods. *R news* **7**: 47–52.
- Dray, S., P. Choler, S. Dolédec, P. R. Peres-Neto, W. Thuiller, S. Pavoine, and C. J. F. ter Braak. 2014. Combining the fourth-corner and the RLQ methods for assessing trait responses to environmental variation. *Ecology* **95**: 14–21. doi:[10.1890/13-0196.1](https://doi.org/10.1890/13-0196.1)
- Fagherazzi, S., and others. 2013. 12.13 Ecogeomorphology of tidal flats, p. 201–220. *In* J. F. Shroder [ed.], *Treatise on geomorphology*. Academic Press.
- FitzGerald, D. M., M. S. Fenster, B. A. Argow, and I. V. Buynevich. 2008. Coastal impacts due to sea-level rise. *Annu. Rev. Earth Planet. Sci.* **36**: 601–647. doi:[10.1146/annurev.earth.35.031306.140139](https://doi.org/10.1146/annurev.earth.35.031306.140139)
- Fu, X., W. Yang, L. Zheng, D. Liu, and X. Li. 2022. Spatial patterns of macrobenthos taxonomic and functional diversity throughout the ecotones from river to lake: A case study in Northern China. *Front. Ecol. Evol.* **10**: 922539. doi:[10.3389/fevo.2022.922539](https://doi.org/10.3389/fevo.2022.922539)
- Garland, T. 2014. Trade-offs. *Curr. Biol.* **24**: R60–R61. doi:[10.1016/j.cub.2013.11.036](https://doi.org/10.1016/j.cub.2013.11.036)
- Garwood, J. C., P. S. Hill, H. L. MacIntyre, and B. A. Law. 2015. Grain sizes retained by diatom biofilms during erosion on tidal flats linked to bed sediment texture. *Cont. Shelf Res.* **104**: 37–44. doi:[10.1016/j.csr.2015.05.004](https://doi.org/10.1016/j.csr.2015.05.004)
- Grandjean, T. J., J. C. de Smit, J. van Belzen, G. S. Fivash, J. van Dalen, T. Ysebaert, and T. J. Bouma. 2023. Morphodynamic signatures derived from daily surface elevation dynamics can explain the morphodynamic development of tidal flats. *Water Sci. Eng.* **16**: 14–25. doi:[10.1016/j.wse.2022.11.003](https://doi.org/10.1016/j.wse.2022.11.003)
- Gravina, M. F., A. Bonifazi, M. Del Pasqua, J. Giampaolletti, M. Lezzi, D. Ventura, and A. Giangrande. 2020. Perception of changes in marine benthic habitats: The relevance of taxonomic and ecological memory. *Diversity* **12**: 480. doi:[10.3390/d12120480](https://doi.org/10.3390/d12120480)
- Gu, H., J. Hughes, and S. Dorn. 2006. Trade-off between mobility and fitness in *Cydia pomonella* L. (Lepidoptera: Tortricidae). *Ecol. Entomol.* **31**: 68–74. doi:[10.1111/j.0307-6946.2006.00761.x](https://doi.org/10.1111/j.0307-6946.2006.00761.x)
- Hinkel, J., and others. 2014. Coastal flood damage and adaptation costs under 21st century sea-level rise. *Proc. Natl. Acad. Sci. USA* **111**: 3292–3297. doi:[10.1073/pnas.1222469111](https://doi.org/10.1073/pnas.1222469111)
- Hu, Z., P. Yao, D. Van Der Wal, and T. J. Bouma. 2017. Patterns and drivers of daily bed-level dynamics on two tidal flats with contrasting wave exposure. *Sci. Rep.* **7**: 7088. doi:[10.1038/s41598-017-07515-y](https://doi.org/10.1038/s41598-017-07515-y)
- Janssen, M., L. Lemke, and J. Miller. 2019. Application of Storm Erosion Index (SEI) to parameterize spatial storm intensity and impacts from Hurricane Michael. *Shore Beach* **41–50**: 41–50. doi:[10.34237/1008745](https://doi.org/10.34237/1008745)
- Jennings, S., and M. J. Kaiser. 1998. The effects of fishing on marine ecosystems, p. 201–352. *In* *Advances in marine biology*. Elsevier.
- Johnstone, J. F., and others. 2016. Changing disturbance regimes, ecological memory, and forest resilience. *Front. Ecol. Environ.* **14**: 369–378. doi:[10.1002/fee.1311](https://doi.org/10.1002/fee.1311)
- Jonsson, I. G., and N. A. Carlsen. 1976. Experimental and theoretical investigations in an oscillatory turbulent boundary layer. *J. Hydraul. Res.* **14**: 45–60. doi:[10.1080/00221687609499687](https://doi.org/10.1080/00221687609499687)
- Kristensen, E., G. Penha-Lopes, M. Delefosse, T. Valdemarsen, C. Quintana, and G. Banta. 2012. What is bioturbation? The need for a precise definition for fauna in aquatic sciences. *Mar. Ecol. Prog. Ser.* **446**: 285–302. doi:[10.3354/meps09506](https://doi.org/10.3354/meps09506)
- Le Hir, P., Y. Monbet, and F. Orvain. 2007. Sediment erodability in sediment transport modelling: Can we account for biota effects? *Cont. Shelf Res.* **27**: 1116–1142. doi:[10.1016/j.csr.2005.11.016](https://doi.org/10.1016/j.csr.2005.11.016)

- Lebreton, J.-D., R. Sabatier, G. Banco, and A.-M. Bacou. 1991. Principal component and correspondence analyses with respect to instrumental variables: An overview of their role in studies of structure–activity and species–environment relationships, p. 85–114. *In* J. Devillers and W. Karcher [eds.], Applied multivariate analysis in SAR and environmental studies. Springer.
- Lewis, L. J., J. Davenport, and T. C. Kelly. 2003. A study of the impact of a pipeline construction on estuarine benthic invertebrate communities. *Estuar. Coast. Shelf Sci.* **57**: 201–208. doi:[10.1016/S0272-7714\(02\)00345-1](https://doi.org/10.1016/S0272-7714(02)00345-1)
- MacDonald, E. C., E. H. Frost, S. M. MacNeil, D. J. Hamilton, and M. A. Barbeau. 2014. Behavioral response of *Corophium volutator* to shorebird predation in the Upper Bay of Fundy, Canada. *PLoS One* **9**: e110633. doi:[10.1371/journal.pone.0110633](https://doi.org/10.1371/journal.pone.0110633)
- McLachlan, A. 1980. The definition of sandy beaches in relation to exposure: A simple rating system. *S. Afr. J. Sci.* **76**: 137–138.
- McLachlan, A., and O. Defeo. 2018a. Adaptations to Sandy-beach life, p. 103–138. *In* The ecology of Sandy shores. Elsevier.
- McLachlan, A., and O. Defeo. 2018b. Benthic macrofauna communities, p. 139–191. *In* The ecology of Sandy shores. Elsevier.
- McLachlan, A., O. Defeo, and A. D. Short. 2018. Characterising sandy beaches into major types and states: Implications for ecologists and managers. *Estuar. Coast. Shelf Sci.* **215**: 152–160. doi:[10.1016/j.ecss.2018.09.027](https://doi.org/10.1016/j.ecss.2018.09.027)
- Meire, P. M., H. Schekkerman, and P. L. Meininger. 1994. Consumption of benthic invertebrates by waterbirds in the Oosterschelde estuary, SW Netherlands. *Hydrobiologia* **282**: 525–546.
- Meysman, F., J. Middelburg, and C. Heip. 2006. Bioturbation: A fresh look at Darwin's last idea. *Trends Ecol. Evol.* **21**: 688–695. doi:[10.1016/j.tree.2006.08.002](https://doi.org/10.1016/j.tree.2006.08.002)
- Morys, C., S. Forster, and G. Graf. 2016. Variability of bioturbation in various sediment types and on different spatial scales in the southwestern Baltic Sea. *Mar. Ecol. Prog. Ser.* **557**: 31–49. doi:[10.3354/meps11837](https://doi.org/10.3354/meps11837)
- Mueter, F. J., and others. 2021. Possible future scenarios in the gateways to the Arctic for subarctic and Arctic marine systems: II. Prey resources, food webs, fish, and fisheries. *ICES J. Mar. Sci.* **78**: 3017–3045. doi:[10.1093/icesjms/fsab122](https://doi.org/10.1093/icesjms/fsab122)
- Murray, J. M. H., A. Meadows, and P. S. Meadows. 2002. Biogeomorphological implications of microscale interactions between sediment geotechnics and marine benthos: A review. *Geomorphology* **47**: 15–30. doi:[10.1016/S0169-555X\(02\)00138-1](https://doi.org/10.1016/S0169-555X(02)00138-1)
- Naeem, S., L. J. Thompson, S. P. Lawler, J. H. Lawton, and R. M. Woodfin. 1994. Declining biodiversity can alter the performance of ecosystems. *Nature* **368**: 734–737.
- Nolte, S., E. C. Koppelaar, P. Esselink, K. S. Dijkema, M. Schuerch, A. V. De Groot, J. P. Bakker, and S. Temmerman. 2013. Measuring sedimentation in tidal marshes: A review on methods and their applicability in biogeomorphological studies. *J. Coast. Conserv.* **17**: 301–325. doi:[10.1007/s11852-013-0238-3](https://doi.org/10.1007/s11852-013-0238-3)
- O'Brien, K. R., and others. 2018. Seagrass ecosystem trajectory depends on the relative timescales of resistance, recovery and disturbance. *Mar. Pollut. Bull.* **134**: 166–176. doi:[10.1016/j.marpolbul.2017.09.006](https://doi.org/10.1016/j.marpolbul.2017.09.006)
- O'Donoghue, T., and G. S. Clubb. 2001. Sand ripples generated by regular oscillatory flow. *Coastal Eng.* **44**: 101–115. doi:[10.1016/S0378-3839\(01\)00025-4](https://doi.org/10.1016/S0378-3839(01)00025-4)
- Pagès, J. F., A. Gera, J. Romero, S. Farina, A. Garcia-Rubies, B. Hereu, and T. Alcoverro. 2013. The Mediterranean benthic herbivores show diverse responses to extreme storm disturbances. *PLoS One* **8**: e62719. doi:[10.1371/journal.pone.0062719](https://doi.org/10.1371/journal.pone.0062719)
- Pelegri, S. P., and T. H. Blackburn. 1994. Bioturbation effects of the amphipod *Corophium volutator* on microbial nitrogen transformations in marine sediments. *Mar. Biol.* **121**: 253–258. <https://doi.org/10.1007/bf00346733>
- Poole, W. C., and K. W. Stewart. 1976. The vertical distribution of macrobenthos within the substratum of the Brazos river, Texas. *Hydrobiologia* **50**: 151–160. doi:[10.1007/BF00019818](https://doi.org/10.1007/BF00019818)
- Queirós, A. M., and others. 2013. A bioturbation classification of European marine infaunal invertebrates. *Ecol. Evol.* **3**: 3958–3985. doi:[10.1002/ece3.769](https://doi.org/10.1002/ece3.769)
- R Core Team. 2023. R: A language and environment for statistical computing. R Foundation for Statistical Computing.
- Ribberink, J. S., J. J. van der Werf, T. O'Donoghue, and W. N. M. Hassan. 2008. Sand motion induced by oscillatory flows: Sheet flow and vortex ripples. *J. Turbul.* **9**: N20. doi:[10.1080/14685240802220009](https://doi.org/10.1080/14685240802220009)
- Romano, C., G. Sara, G. Salvo, J. Bishop, A. Mazzola, and J. Widdows. 2011. Effect of the presence of the shore crab, *Carcinus maenas*, on burrowing behaviour and clearance rate of the common cockle, *Cerastoderma edule*. *Mar. Biol.* **158**: 2685–2694. doi:[10.1007/s00227-011-1766-8](https://doi.org/10.1007/s00227-011-1766-8)
- Shi, B., and others. 2021. Effect of typhoon-induced intertidal-flat erosion on dominant macrobenthic species (*Meretrix meretrix*). *Limnol. Oceanogr.* **66**: 4197–4209. doi:[10.1002/lno.11953](https://doi.org/10.1002/lno.11953)
- Shoval, O., and others. 2012. Evolutionary trade-offs, pareto optimality, and the geometry of phenotype space. *Science* **336**: 1157–1160. doi:[10.1126/science.1217405](https://doi.org/10.1126/science.1217405)
- Soissons, L. M., T. Gomes da Conceição, J. Bastiaan, J. van Dalen, T. Ysebaert, P. M. J. Herman, F. Cozzoli, and T. J. Bouma. 2019. Sandification vs. muddification of tidal flats by benthic organisms: A flume study. *Estuar. Coast. Shelf Sci.* **228**: 106355. doi:[10.1016/j.ecss.2019.106355](https://doi.org/10.1016/j.ecss.2019.106355)
- ter Braak, C. J. 1986. Canonical correspondence analysis: A new eigenvector technique for multivariate direct gradient analysis. *Ecology* **67**: 1167–1179.
- Thioulouse, J., S. Dray, A.-B. Dufour, A. Siberchicot, T. Jombart, and S. Pavoine. 2018. Multivariate analysis of ecological data with ade4. Springer.

- Thrush, S. F., R. B. Whitlatch, R. D. Pridmore, J. E. Hewitt, V. J. Cummings, and M. R. Wilkinson. 1996. Scale-dependent recolonization: The role of sediment stability in a dynamic sandflat habitat. *Ecology* **77**: 2472–2487. doi:[10.2307/2265747](https://doi.org/10.2307/2265747)
- Turner, M. G. 2010. Disturbance and landscape dynamics in a changing world. *Ecology* **91**: 2833–2849. doi:[10.1890/10-0097.1](https://doi.org/10.1890/10-0097.1)
- Turner, M. G., and others. 2020. Climate change, ecosystems and abrupt change: Science priorities. *Philos. Trans. R. Soc. B* **375**: 20190105. doi:[10.1098/rstb.2019.0105](https://doi.org/10.1098/rstb.2019.0105)
- Ummenhofer, C. C., and G. A. Meehl. 2017. Extreme weather and climate events with ecological relevance: A review. *Philos. Trans. R. Soc. Lond. B Biol. Sci.* **372**: 20160135. doi:[10.1098/rstb.2016.0135](https://doi.org/10.1098/rstb.2016.0135)
- van Belzen, J., G. S. Fivash, Z. Hu, T. J. Bouma, and P. M. J. Herman. 2022. A probabilistic framework for windows of opportunity: The role of temporal variability in critical transitions. *J. R. Soc. Interface* **19**: 20220041. doi:[10.1098/rsif.2022.0041](https://doi.org/10.1098/rsif.2022.0041)
- van de Koppel, J., P. M. J. Herman, P. Thoolen, and C. H. R. Heip. 2001. Do alternate stable states occur in natural ecosystems? Evidence from a tidal flat. *Ecology* **82**: 3449–3461. doi:[10.1890/0012-9658\(2001\)082\[3449:DASSOI\]2.0.CO;2](https://doi.org/10.1890/0012-9658(2001)082[3449:DASSOI]2.0.CO;2)
- van der Linden, P., J. Patrício, A. Marchini, N. Cid, J. M. Neto, and J. C. Marques. 2012. A biological trait approach to assess the functional composition of subtidal benthic communities in an estuarine ecosystem. *Ecol. Indic.* **20**: 121–133. doi:[10.1016/j.ecolind.2012.02.004](https://doi.org/10.1016/j.ecolind.2012.02.004)
- van der Wal, D., G. I. Lambert, T. Ysebaert, Y. M. G. Plancke, and P. M. J. Herman. 2017. Hydrodynamic conditioning of diversity and functional traits in subtidal estuarine macrozoobenthic communities. *Estuar. Coast. Shelf Sci.* **197**: 80–92. doi:[10.1016/j.ecss.2017.08.012](https://doi.org/10.1016/j.ecss.2017.08.012)
- Walles, B., J. Salvador de Paiva, B. C. van Prooijen, T. Ysebaert, and A. C. Smaal. 2015. The ecosystem engineer *Crassostrea gigas* affects tidal flat morphology beyond the boundary of their reef structures. *Estuar. Coasts* **38**: 941–950. doi:[10.1007/s12237-014-9860-z](https://doi.org/10.1007/s12237-014-9860-z)
- Weston, D. 1990. Quantitative examination of macrobenthic community changes along an organic enrichment gradient. *Mar. Ecol. Prog. Ser.* **61**: 233–244. doi:[10.3354/meps061233](https://doi.org/10.3354/meps061233)
- Willemsen, P. W. J. M., E. M. Horstman, T. J. Bouma, M. J. Baptist, M. E. B. van Puijenbroek, and B. W. Borsje. 2022. Facilitating salt marsh restoration: The importance of event-based bed level dynamics and seasonal trends in bed level change. *Front. Mar. Sci.* **8**: 793235. doi:[10.3389/fmars.2021.793235](https://doi.org/10.3389/fmars.2021.793235)
- WoRMS Editorial Board. 2024. World Register of Marine Species; [accessed 2024 August 31]. Available from <https://www.marinespecies.org> at VLIZ
- Wright, J. P., and C. G. Jones. 2006. The concept of organisms as ecosystem engineers ten years on: Progress, limitations, and challenges. *Bioscience* **56**: 203. doi:[10.1641/0006-3568\(2006\)056\[0203:TCOOAE\]2.0.CO;2](https://doi.org/10.1641/0006-3568(2006)056[0203:TCOOAE]2.0.CO;2)
- Ysebaert, T., and P. Herman. 2002. Spatial and temporal variation in benthic macrofauna and relationships with environmental variables in an estuarine, intertidal soft-sediment environment. *Mar. Ecol. Prog. Ser.* **244**: 105–124. doi:[10.3354/meps244105](https://doi.org/10.3354/meps244105)
- Zhu, Z., J. Belzen, Q. Zhu, J. Koppel, and T. J. Bouma. 2020. Vegetation recovery on neighboring tidal flats forms an Achilles' heel of saltmarsh resilience to sea level rise. *Limnol. Oceanogr.* **65**: 51–62. doi:[10.1002/lno.11249](https://doi.org/10.1002/lno.11249)

#### Conflict of Interest

The authors declare no conflicts of interest.

Submitted 21 July 2023

Revised 06 March 2024

Accepted 05 August 2024

Associate editor: Josef D. Ackerman